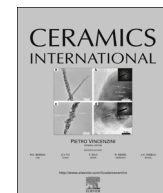




Contents lists available at ScienceDirect

Ceramics International

journal homepage: www.elsevier.com/locate/ceramint

Influence of $\text{La}_2\text{O}_3/\text{SrO}$ doping of $(\text{Zr}_{0.8}\text{Sn}_{0.2})\text{TiO}_4$ ceramics on their sintering behavior and microwave dielectric properties

Qinglei Sun ^{a,b}, Hongqing Zhou ^{a,b,*}, Xianfu Luo ^{a,b}, Lisong Hu ^{a,b}, Luchao Ren ^{a,b}^a College of Materials Science and Engineering, Nanjing Tech University, Nanjing 210009, China^b Jiangsu Collaborative Innovation Center for Advanced Inorganic Function Composites, Nanjing 210009, China

ARTICLE INFO

Article history:

Received 29 February 2016

Received in revised form

29 April 2016

Accepted 1 May 2016

Keywords:

- A. Sintering behavior
 - B. Microstructures
 - C. Dielectric properties
- $(\text{Zr}_{0.8}\text{Sn}_{0.2})\text{TiO}_4$ ceramics

ABSTRACT

The phase formation, microstructures, sintering behavior and microwave dielectric properties of $(\text{Zr}_{0.8}\text{Sn}_{0.2})\text{TiO}_4$ (ZST) ceramics with different amounts of $\text{La}_2\text{O}_3/\text{SrO}$ additives, fabricated by the conventional solid-state reaction route, were systematically investigated. Single-phase orthorhombic crystalline structure was detected in the X-ray diffraction patterns, and the $\text{La}_2\text{O}_3/\text{SrO}$ additives were found to effectively reduce the sintering temperature of ZST ceramics to 1310 °C and improve the microwave dielectric properties as long as they were supplemented in the appropriate amount (0.25 wt% La_2O_3 and 0.5 wt% SrO). Low cooling rate created significant improvement in the microwave dielectric properties of the ZST ceramics. A maximum $Q \times f$ of 41,000 GHz (at 5.6 GHz) associated with an ϵ_r of 39.56 and a τ_f of -2.65 ppm/°C was achieved for ZST ceramics with 0.25 wt% La_2O_3 and 0.5 wt% SrO sintered at 1310 °C for 5 h.

© 2016 Published by Elsevier Ltd.

1. Introduction

Alongside significant advancements in microwave communication, such as 4G/5G, non-compressed digital video transmission systems, wireless local area networks, and the carrier frequencies of signals extending to higher frequency bands, the production of dielectric resonators has provided a powerful impetus to explore new dielectric materials to satisfy the demands for electronic devices that function in microwave and millimeter wave regions [1–4].

In this regard, $(\text{Zr}_{0.8}\text{Sn}_{0.2})\text{TiO}_4$ (ZST) ceramics are popularly utilized in wireless communication system microwave devices by virtue of their high dielectric constants ($\epsilon_r > 25$), which facilitate miniaturization and integration of the passive circuits. There also are certain high quality factors ($Q > 5000$) which allow rapid electronic signal transition at ultra-high frequencies and near-zero temperature coefficients of resonant frequency ($\tau_f < \pm 10 \text{ ppm}/\text{°C}$) which guarantee the temperature stability of the devices. The high sintering temperature (1400–1450 °C) necessary to process these ceramics, however, limits their practical application [5–8]. A number of strategies can be used to investigate the sintering temperature and microwave properties of ZST ceramics via adding minor dopants, (e.g., La_2O_3 , ZnO , SrO and CuO) [9–12]. These additives do effectively reduce the sintering temperature of ZST

ceramics and thereby the cost of production without deteriorating their dielectric performance. In a previous study, Zhang et al. [9] synthesized ZST ceramics by adding 1 wt% La_2O_3 and 2 wt% BaO to form material with comprehensive performance of $\rho = 5.10 \text{ g/cm}^3$, $\epsilon_r = 41$, $Q = 9800$ and $\tau_f = -3.79 \text{ ppm}/\text{°C}$ when sintered at 1350 °C. Pamu et al. [11] reported that the sintering temperature of ZST ceramics doped with 0.5 wt% SrO and 1 wt% ZnO can be decreased to 1350 °C, with resultant dielectric properties of $\epsilon_r = 37$ and $Q \times f = 54,250 \text{ GHz}$ (at 11.94 GHz), $\tau_f = 6.2 \text{ ppm}/\text{°C}$.

A liquid-phase effect is believed to be the cause of increased sinterability introduced by the eutectic of $\text{La}_2\text{O}_3/\text{TiO}_2$ at 1400 °C. The addition of SrO does not affect the dielectric constant (ϵ_r) or temperature coefficient of resonant frequency (τ_f), and can improve the quality of the material [13]. Nevertheless, La_2O_3 and SrO have not yet been used as sintering aids in ZST ceramics. In this study, we systematically investigate the influence of $\text{La}_2\text{O}_3/\text{SrO}$ additives on the phase composition, microstructures, sinterability, and microwave dielectric properties of ZST ceramics to find that the additives provide excellent temperature stability of the resonant frequency to the material. We also examine the effect of cooling rate on microwave dielectric properties of ZST ceramics, as discussed below.

2. Experimental procedure

Samples of ZST ceramics were synthesized using conventional solid-state methods from dried high-purity oxide powders: ZrO_2

* Correspondence to: College of Materials Science and Engineering, Nanjing Tech University, No.5 New Mofan Road, Nanjing 210009, Jiangsu, China.

E-mail address: hqzhou@njtech.edu.cn (H. Zhou).

Table 1
wt% of additives in ZST ceramics.

Sample designation	La ₂ O ₃ (wt%)	SrO (wt%)	Total additives (wt%)
LS075	0.25	0.5	0.75
LS150	0.5	1.0	1.5
LS225	0.75	1.5	2.25
LS300	1.0	2.0	3.0

(99.9%, Farmeiya Co., Ltd., Jiangxi, China, the average particle size ca. 0.591 μm), SnO₂ (99.9%, Tin Co., Ltd. Yunnan, China, the average particle size ca. 0.491 μm), TiO₂ (99.5%, Pengbo Titanium Dioxide Co., Ltd., Shanghai, China, the average particle size ca. 0.580 μm) and La₂O₃ (99.9%, Luodiya Rare Earth New Materials Co., Ltd., Jiangsu, China, the average particle size ca. 1.802 μm). The starting materials were mixed according to the desired stoichiometry of (Zr_{0.8}Sn_{0.2})TiO₄ ceramics. After grounding under distilled water for 24 h in a ball mill with zirconia balls, the mixtures were dried, forced through a 100-mesh sieve, and then calcined at 1100 °C for 2 h. To obtain SrO, SrCO₃ (99.9%, Reagent No.1 Factory of Shanghai Chemical Reagent Co., Ltd., Shanghai, China, the average particle size ca. 5.754 μm) powders were calcined at 1200 °C for 6 h. The weight percent of La₂O₃/SrO additives are tabulated in Table 1. The ratio of La₂O₃ and SrO was kept as 1–2 in all samples. The calcined powders were mixed as desired composition with various amounts of La₂O₃ and SrO as sintering aids and re-milled with zirconia balls for 8 h in distilled water and dried. The dried powders with 8 wt% of a 7% solution of PVA as a binder were screened by a 150-mesh. The final powders were pressed uniaxially under 150 MPa into disk pellets with a diameter of 13 mm and thickness of 7 mm. The pellets were sintered in air at temperatures ranging from 1250 to 1370 °C for 5 h with a heating rate of 180 °C/h and cooling rate of 180 °C/h. Selected samples were also cooled at 120, 60 and 30 °C/h.

The bulk densities of the sintered ceramics were measured using the Archimedes method. Crystalline phases of sintered samples were identified by means of the X-ray powder diffraction (XRD; RIGAKU; Smartlab 3) with CuKα radiation from 20° to 70° in 2θ. The scanning rate was 10 °/min. The microstructures were observed and analyzed using a scanning electron microscope (SEM, JEOL, JSM-5900). Flexure strength of the ceramics was measured by three-point bending method according to RGWT-4002 using a universal testing machine with a 30 mm span and a displacement speed of 0.5 mm/min at the ambient temperature in air. All testing specimens were rectangular bars of 4 mm × 6 mm × 50 mm³ in size. The dielectric constants (ε_r) and unloaded Q values at microwave frequencies were measured using the Hakki–Coleman dielectric resonator method. The temperature coefficient of resonant frequency (τ_f) was calculated in the temperature range of 25–80 °C. The τ_f (ppm/°C) was calculated by noting the change in resonant frequency:

$$\tau_f = \frac{1}{f_{25}} \times \frac{f_{80} - f_{25}}{80 - 25} \quad (1)$$

where f₈₀ was the resonant frequency at 80 °C and f₂₅ was the resonant frequency at 25 °C.

3. Results and discussion

3.1. X-ray diffraction analysis

Fig. 1 illustrates the X-ray diffraction patterns of ZST ceramics sintered at 1310 °C prepared with different levels of La₂O₃/SrO additives. All samples show a homogeneous phase with α-PbO₂

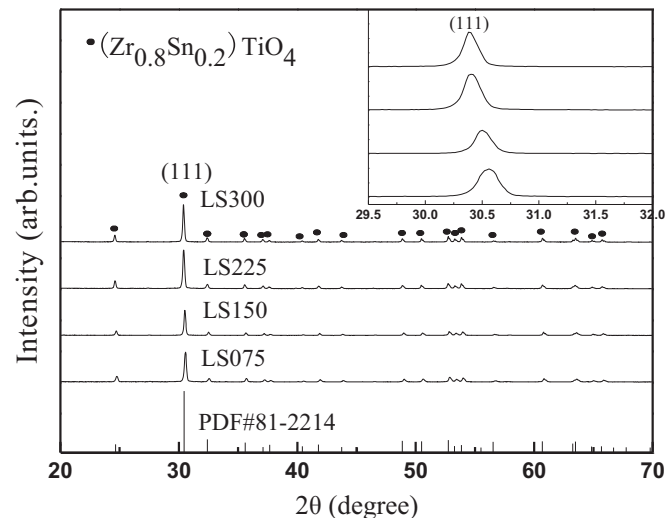


Fig. 1. X-ray diffraction patterns of ZST ceramics sintered at 1310 °C with different amounts of La₂O₃/SrO additives.

orthorhombic structure (JCPDS Card no. 81–2214) and the structure space group D142h = Pbca. It is commonly accepted that La₂O₃ forms a secondary phase at the grain boundary, but we observe no such minor phase in the XRD patterns because detection of minor secondary phases using XRD is extremely intractable. We also investigate the doping mechanism of ZST ceramics according to the (111) peaks shown in the inset in Fig. 1, the lattice parameters and unit cell volume listed in Table 2 are calculated according to these peaks. The (111) peaks shift to a lower angle gradually as the amounts of La₂O₃/SrO additives increase, while the lattice parameters and unit cell volume of ZST ceramics increase substantially. These results are due to the differences in ionic sizes between the substitution ions and the tetravalent ions in ZST ceramics. To be precise, the La³⁺ and Sr²⁺ could not be substituted for the tetravalent ZST ceramics elements due to the fact that the ionic radii of La³⁺ (1.032 Å) and Sr²⁺ (1.18 Å) are much larger than Zr⁴⁺ (0.72 Å), Sn⁴⁺ (0.69 Å), and Ti⁴⁺ (0.61 Å) ions. Increasing La₂O₃/SrO additions enlarge the interplanar distance (according to the Bragg equation), and ultimately make the unit cell expand. A similar study by Zhu et al. [14] yields similar results.

3.2. Scanning electron micrograph

Typical SEM micrographs of the fractured surfaces of the well-sintered ZST ceramics with different amounts of La₂O₃/SrO additives sintered at 1310 °C are depicted in Fig. 2 (a) to (d). Dense microstructures with few microcracks are observed in all compositions. The grain size is greater and the size distribution is relatively uniform for LS075 compared to other compositions. The appropriate liquid phase provides a faster transport path for diffusion, thus enhancing homogenization and densification processes to promote grain growth as shown in Fig. 2(a). The average

Table 2
Calculated lattice parameters and unit cell volume for ZST ceramics.

Composition	Sintering	Lattice parameters			Unit cell volume (Å ³)	
		temperature (°C)	a ₀ (Å)	b ₀ (Å)	c ₀ (Å)	
LS075	1310		0.4806	0.5032	0.5448	131.75
LS150	1310		0.4807	0.5047	0.5479	132.93
LS225	1310		0.4768	0.5156	0.5578	137.13
LS300	1310		0.4765	0.5256	0.5613	140.58

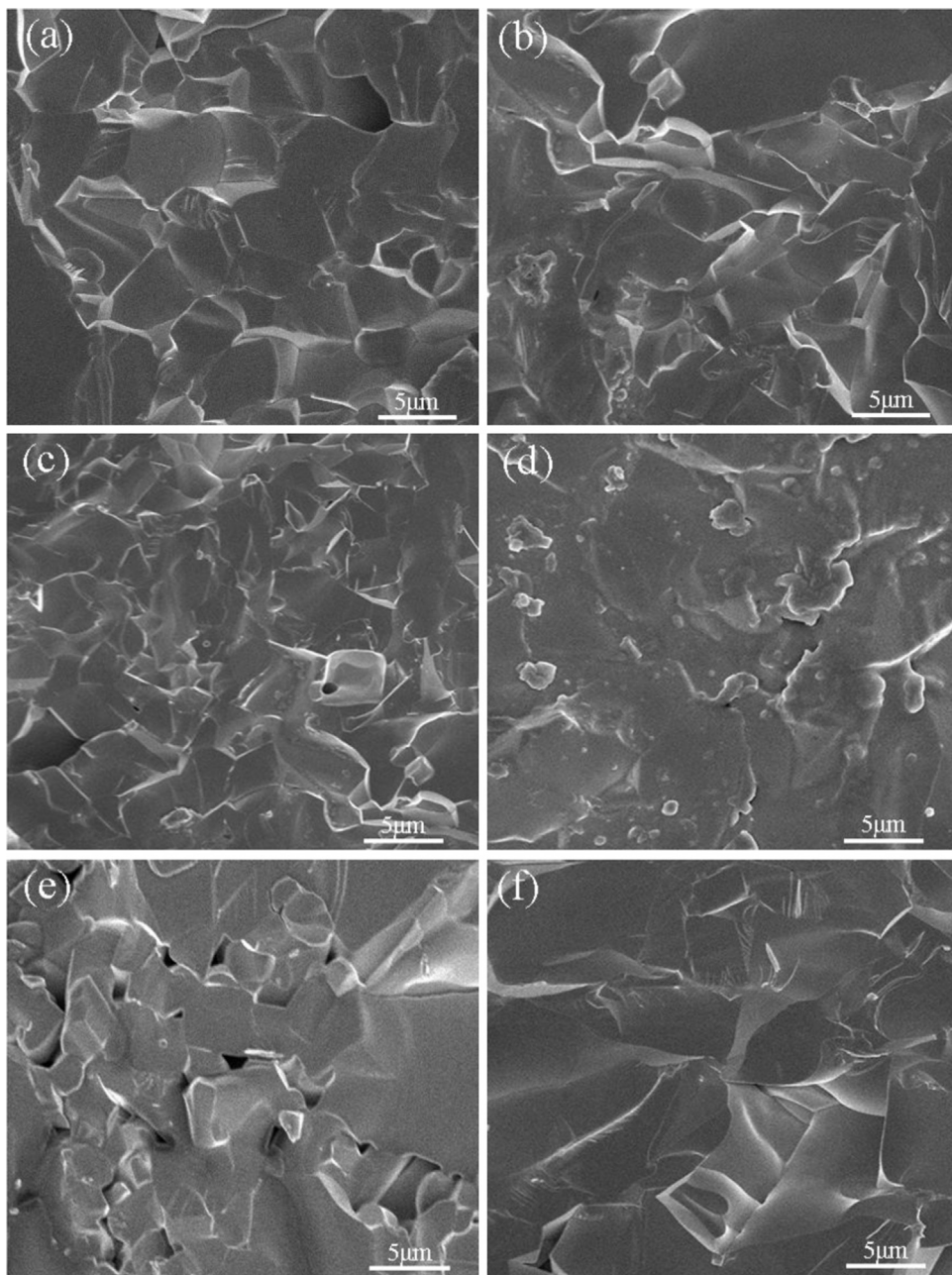


Fig. 2. SEM micrographs on fractured surfaces of ZST ceramics with (a) LS075, (b) LS150, (c) LS225, (d) LS300 sintered at 1310 °C, (e) LS075 sintered at 1250 °C, (f) LS075 sintered at 1370 °C.

grain size of ZST ceramics evidently decreases as $\text{La}_2\text{O}_3/\text{SrO}$ additions increase, where the excessive liquid phase deteriorates ceramics densification and inhibits grain growth due to high surface energy [15]. Further, the samples show irregular variations in grain growth and non-uniform distribution as the amounts of $\text{La}_2\text{O}_3/\text{SrO}$ additives increase, as shown in Fig. 2(c) and (d). Typical SEM micrographs of fractured surfaces for LS075 sintered at different temperatures are shown in Fig. 2(e) and (f). Compared to LS075, which is sintered at 1310 °C, insufficient sintering temperature (1250 °C) lowers the driving force for densification and inhibits the extraction of pores from the ceramics, increasing intragranular pores in the material [16]. Taken together, these observations suggest ensuring the appropriate amount of additives plays an important role in the densification, grain growth, and grain size of ZST ceramics.

3.3. Sintered density

Fig. 3 demonstrates the bulk densities (ρ) of ZST ceramics with various amounts of $\text{La}_2\text{O}_3/\text{SrO}$ additives versus various sintering temperatures. The bulk densities decrease as amounts of $\text{La}_2\text{O}_3/\text{SrO}$ additives increase in all the samples observed, while the bulk densities initially increase with increasing sintering temperature and then drop after reaching a maximum value, which allows us to determine the optimal sintering temperature (1310 °C) for all samples. The samples show maximum bulk densities of 98.27%, 97.30%, 96.15%, and 94.61% of the nominal theoretical density (5.19 g/cm³ for pure ZST) at 1310 °C for LS075, LS150, LS225, and LS300, respectively. The optimal bulk density may have appeared due to the scarcity of pores and uniform grain growth having decreased the grain boundary area, as shown in Fig. 2(a). Larger additive contents result in lower bulk densities, so

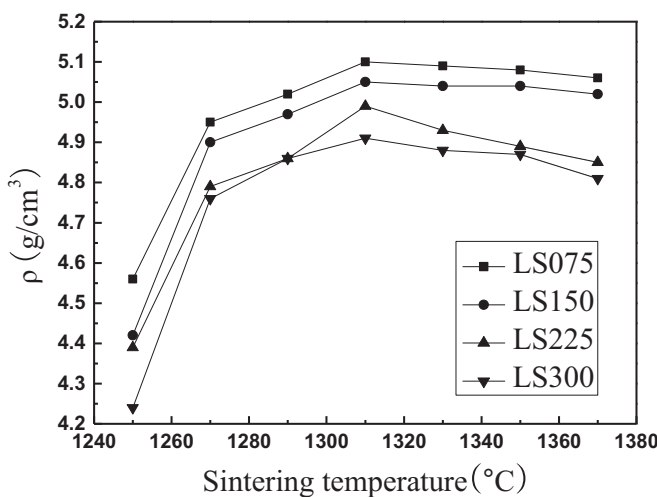


Fig. 3. Bulk densities (ρ) of ZST ceramics with various amounts of $\text{La}_2\text{O}_3/\text{SrO}$ additives as a function of sintering temperature.

reduction in density can be attributed to intergranular porosity and inhomogeneous liquid phase effect, which cause decreased grain size. Intergranular porosity and a heterogeneous microstructure could be seen in SEM micrographs of the selected samples (Fig. 2(c) and (d)), in which decreased grain uniformity results in reduced density.

3.4. Microwave dielectric properties

Fig. 4 depicts the dielectric constants (ϵ_r) of ZST ceramics with different amounts of $\text{La}_2\text{O}_3/\text{SrO}$ additives, supplemented as functions of their sintering temperatures. We find that the dielectric constants first increase as sintering temperature increase, reaching the maximum at 1310 °C, then continually decline thereafter. The dielectric constants of ZST ceramics range from 29.79 to 39.56 as the sintering temperature increases from 1250 to 1370 °C, and a maximum ϵ_r value of 39.56 for LS075 is achieved at 1310 °C, indicating that further increase in sintering temperature does not necessarily lead to a higher dielectric constant. Dielectric constants are instead dependent on bulk densities, secondary phases, and crystal structures in the microwave frequency [17]. In present work, the dielectric constants of ZST ceramics with different sintering temperature are observed to be dependent on the bulk densities because no secondary phases exist and no structures

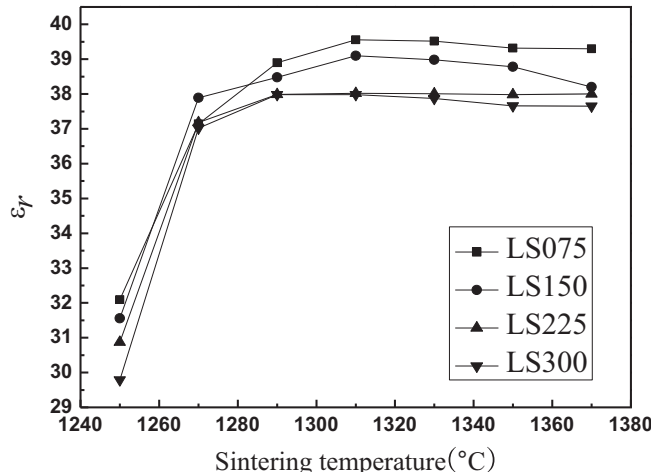


Fig. 4. Dielectric constants (ϵ_r) of ZST ceramics with various amounts of $\text{La}_2\text{O}_3/\text{SrO}$ additives as a function of sintering temperature.

change. In all the cases, we observed that the relationship between dielectric constants and additive contents reveals the same trend in the relation between bulk densities and additive contents. It is commonly known that dielectric constants vary with the total molecular dielectric polarizability and molar volume according to the Clausius–Mossotti equation [18]. Therefore, the dielectric constants of $\text{La}_2\text{O}_3/\text{SrO}$ doping of ZST ceramics are larger than that of pure ZST ceramics (Table 3) because of the ionic dielectric polarizabilities of La^{3+} (6.07 \AA^3) and Sr^{2+} ions (4.24 \AA^3) are larger than that of Zr^{4+} (3.25 \AA^3), Sn^{4+} (2.83 \AA^3) and Ti^{4+} (2.93 \AA^3) ions [19]. Additionally, the expansion of the unit cell volume displays in Table 2 causes the dielectric polarizability in the unit cell volume to decrease, which then decreases the dielectric constants of the samples.

The $Q \times f$ values of ZST ceramics with various amounts of $\text{La}_2\text{O}_3/\text{SrO}$ additives as a function of different temperatures are shown in Fig. 5. The $Q \times f$ values first rise with as sintering temperature increases, reaching a maximum value of 41,000 GHz for LS075 at 1310 °C, then drop to around 30,000 GHz for LS225 and LS300 at 1370 °C. Microwave dielectric loss is mainly caused not only by the lattice vibration modes, but also by extended dislocations, densification, grain boundaries, porosity, oxygen vacancies, and secondary phases [20]. Variations in $Q \times f$ values show a similar trend as that of bulk density, which suggests that dielectric loss is mainly related to ceramics densification. In addition, as shown in Fig. 2(a), the grain morphology of LS075 is more uniform and large than other samples. The grain boundary likely decreases the $Q \times f$ values due to plane defects, specimens with uniform and large grains are thus expected to have high $Q \times f$ values because grain growth decreases the grain boundary area, further indicating a reduction in lattice imperfections and dielectric loss [21]. Another important factor in controlling the dielectric loss of ZST ceramics is the possibility of oxygen entrance to the structures, as the introduction of any trivalent impurity increases the oxygen vacancies. Because La^{3+} ions act as an acceptor, the reaction can be expressed as follows:



The decrease in $Q \times f$ values with the increase in addition of La_2O_3 can thus be attributed to the rise in oxygen vacancies, which increases the amount of anharmonic interaction [7].

The dielectric constants (ϵ_r) and $Q \times f$ values for LS075 as a function of cooling rate are plotted in Fig. 6. The dielectric constants and $Q \times f$ values for LS075 are apparently sensitive to cooling rate. Specifically, when samples are cooled at slower rate, the ceramics spend more time at elevated temperatures and as such see a significant improvement in both ϵ_r and $Q \times f$ values. As the cooling rate drops from 180 to 30 °C/h, the dielectric constants increase from 39.56 to 40.11 and the $Q \times f$ values from 40,900 to 42,500 GHz. Cooling rate indeed plays a role in the dielectric properties of ZST ceramics, as a slow cooling process allows local cation ordering to settle [22]. The increase in $Q \times f$ values can also be attributed to the ordering of cations caused by the transformation from a high-temperature structure to a low-temperature structure as cooling rate decreases [23]. In a similar study by Vahabzadeh et al. [24], Ravi et al. [25], annealing and slow cooling are also shown to decrease dielectric loss.

Table 3 summarizes the bulk densities, dielectric properties, and flexure strength of ZST ceramics with different additives. The temperature coefficients of the resonant frequency are -2.65 , -3.70 , -3.84 , and $-3.01 \text{ ppm}/\text{°C}$ for LS075, LS150, LS225, and LS300 sintered at 1310 °C, respectively. There is no significant variation in τ_f observed, implying that dielectric constants of these ceramics have favorable temperature stability in the 25–80 °C. As supported by other results, the temperature coefficients of the

Table 3

Bulk densities, dielectric properties and flexure strength of ZST ceramics with different additives.

Composition	Sintering temperature (°C)	ρ (g/cm ³)	ϵ_r	Q	τ_f (ppm/°C)	Flexure strength (MPa)
Pure ZST [26]	1600	4.92	36.10	7000	0	–
0.5 wt%SrO+1 wt%ZnO [10]	1350	5.02	37.00	4500	+6.2	–
1 wt%La ₂ O ₃ +2.0 wt%BaO [8]	1350	5.10	41.00	9800	-3.79	–
2 wt%La ₂ O ₃ +0.2 wt%MgO+1 wt%ZnO [27]	1320	5.04	36.70	9230	6–7	–
LS075	1310	5.10	39.56	7500	-2.65	101.332
LS150	1310	5.05	39.10	7000	-3.70	90.563
LS225	1310	4.99	38.02	6800	-3.84	84.689
LS300	1310	4.91	37.98	6400	-3.01	69.545

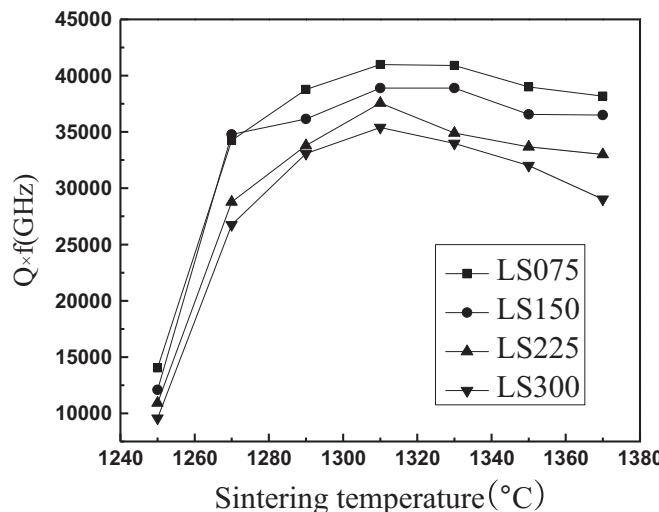


Fig. 5. $Q \times f$ values of ZST ceramics with various amounts of La₂O₃/SrO additives as a function of sintering temperature.

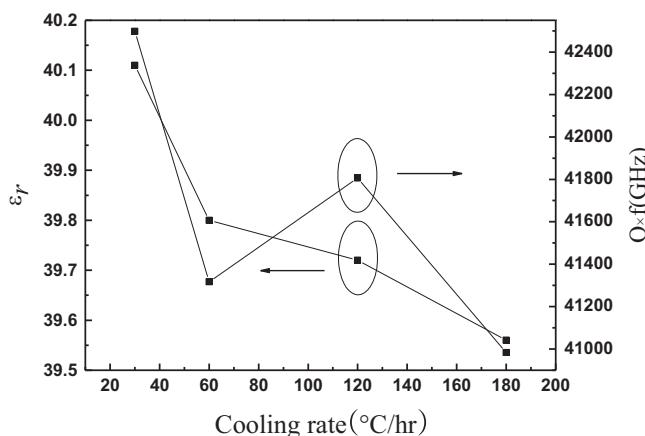


Fig. 6. Dielectric constants (ϵ_r) and $Q \times f$ values for LS075 as a function of cooling rate.

resonant frequency are related to the composition and secondary phases that exist in the ceramics [28]. Because the ZST ceramics are temperature-stable and the La₂O₃/SrO additives do not cause secondary phases, the τ_f values do not change much during the experiment. Clearly, the flexure strength of ZST ceramics dramatically decreases from 101.332 to 69.545 MPa as the amounts of La₂O₃/SrO additives increase. Compared to the microwave dielectric properties of the doped ZST ceramics listed in Table 3, LS075 seems to be the best candidate for dielectric substrate application due to its relatively low sintering temperature of 1310 °C, high dielectric constant of 39.56, high $Q \times f$ value of 41,000 GHz (at 5.6 GHz), and near-zero temperature coefficient of the resonant

frequency, -2.65 ppm/°C.

4. Conclusions

The influence of La₂O₃/SrO additives on the microwave dielectric properties and the microstructures of ZST ceramics are systematically investigated. No secondary phase is detected from X-ray diffraction patterns. The proper additions of La₂O₃/SrO to ZST ceramics are found to significantly improve the density and dielectric properties with reduction in sintering temperature. The samples get densified at 1310 °C with uniform microstructures and few pores. Promising comprehensive performance of $\rho \sim 5.10$ g/cm³, $\epsilon_r \sim 39.56$, $Q \times f$ value $\sim 41,000$ GHz (at 5.6 GHz) and $\tau_f \sim -2.65$ ppm/°C is obtained for ZST ceramics with 0.25 wt% La₂O₃ and 0.5 wt% SrO sintered at 1310 °C for 5 h. We would recommend that this type of ZST ceramics doped with La₂O₃/SrO additives, which show excellent dielectric characteristics and reasonably stable performance at relatively low sintering temperature, be employed for microwave applications that require very low dielectric loss at very high frequencies.

Acknowledgments

The authors are grateful to the support of the fund by the Practice Innovation Program (2015) for University Graduate Students of Jiangsu Province (No. SJZZ15_0095), the Priority Academic Program Development of Jiangsu Higher Education Institution (PAPD), Program for innovative Research Team in University of Ministry of Education of China (IRT_15R35).

Appendix A. Supplementary material

Supplementary data associated with this article can be found in the online version at <http://dx.doi.org/10.1016/j.ceramint.2016.05.002>.

References

- [1] L.J. Cheng, L. Liu, Q. Ma, S.J. Liu, Relationship between densification behavior and stabilization of quasi-liquid grain boundary layers in CuO-doped 0.7CaTiO₃–0.3NdAlO₃ microwave ceramics, Scr. Mater. 111 (2016) 102–105.
- [2] P. Zhang, Y.G. Zhao, Influence of Sm³⁺ substitutions for Nd³⁺ on the microwave dielectric properties of (Nd_{1-x}Sm_x)NbO₄ (x=0.02–0.15) ceramics, J. Alloy. Compd. 654 (2016) 240–245.
- [3] C.F. Tseng, Microwave dielectric properties of low loss microwave dielectric ceramics: A_{0.5}Ti_{0.5}NbO₄ (A=Zn, Co), J. Eur. Ceram. Soc. 34 (15) (2014) 3641–3648.
- [4] S. Wu, K.X. Song, P. Liu, H.X. Lin, F.F. Zhang, P. Zheng, H.B. Qin, Effect of TiO₂ doping on the structure and microwave dielectric properties of cordierite ceramics, J. Am. Ceram. Soc. 98 (6) (2015) 1842–1847.
- [5] S.M. Olhero, A. Kaushal, J.M.F. Ferreira, Fostering the properties of Zr_{0.8}Sn_{0.2}TiO₄ (ZST) ceramics via freeze granulation without sintering additives, RSC Adv. 4 (89) (2014) 48734–48740.

- [6] W.T. Xie, H.Q. Zhou, H.K. Zhu, J.X. Zhao, L.C. Ren, F. Huang, L. Qian, Microwave dielectric properties of $(1-x)\text{Mg}(\text{Sn}_{0.05}\text{Ti}_{0.95})\text{O}_3-x(\text{Ca}_{0.8}\text{Sr}_{0.2})\text{TiO}_3-y$ wt% ZnNb_2O_6 ceramics with near-zero temperature coefficient, *J. Mater. Sci. Mater. Electron.* 26 (6) (2015) 3515–3520.
- [7] R.K. Bhuyan, T.S. Kumar, D. Goswami, A.R. James, D. Pamu, Liquid phase effect of La_2O_3 and V_2O_5 on microwave dielectric properties of Mg_2TiO_4 ceramics, *J. Electroceram.* 31 (1–2) (2013) 48–54.
- [8] Y.Z. Shi, L. Zhang, Z.X. Yue, Dielectric response of $\text{Mg}_{0.95}\text{Ca}_{0.05}\text{TiO}_3$ ceramic filled HDPE composites with low dielectric loss, *Ceram. Int.* 41 (2015) S504–S509.
- [9] S.X. Zhang, J.B. Li, H.Z. Zhai, J.H. Dai, Synthesis and characterization of La_2O_3 /BaO-doped $(\text{Zr}_{0.8}\text{Sn}_{0.2})\text{TiO}_4$ microwave ceramics, *Ceram. Int.* 28 (4) (2002) 407–411.
- [10] L.Z. Wang, L.X. Wang, Z.F. Wang, B.Y. Huang, Q.T. Zhang, Z.X. Fu, Effect of sintering aid $\text{ZnO}-\text{CeO}_2$ on dielectric properties of $(\text{Zr}_{0.8}\text{Sn}_{0.2})\text{TiO}_4$ ceramics, *J. Mater. Sci. Mater. Electron.* 26 (11) (2015) 9026–9030.
- [11] D. Pamu, G.L.N. Rao, K.C.J. Raju, Effect of BaO, SrO and MgO addition on microwave dielectric properties of $(\text{Zr}_{0.8}\text{Sn}_{0.2})\text{TiO}_4$ ceramics, *J. Alloy. Compd.* 475 (1–2) (2009) 745–751.
- [12] D. Pamu, G.L.N. Rao, K.C.J. Raju, M.V. Jacob, Effect of CuO on the sintering and cryogenic microwave characteristics of $(\text{Zr}_{0.8}\text{Sn}_{0.2})\text{TiO}_4$ ceramics, *Sci. Technol. Adv. Mater.* 8 (6) (2007) 469–476.
- [13] D.J. Kim, J.W. Hahn, G.P. Han, S.S. Lee, T.G. Choy, Effects of alkaline-earth-metal addition on the sinterability and microwave characteristics of $(\text{Zr}, \text{Sn})\text{TiO}_4$ dielectrics, *J. Am. Ceram. Soc.* 83 (4) (2000) 1010–1012.
- [14] H.S. Zhu, Z.Y. Cui, C.Y. Shen, Microstructure and microwave dielectric behavior of $0.6\text{ZrO}_2-0.4(\text{Zn}_{1/3}\text{Nb}_{2/3})\text{O}_{2-x}\text{SnO}_{2-y}\text{TiO}_2$ ceramics, *J. Mater. Sci. Mater. Electron.* 27 (1) (2016) 177–181.
- [15] C.L. Huang, M.H. Weng, C.C. Wu, C.C. Wei, Microwave dielectric properties and microstructures of V_2O_5 -modified $\text{Zr}_{0.8}\text{Sn}_{0.2}\text{TiO}_4$ ceramics, *Jpn. J. Appl. Phys.* 40 (2A) (2001) 698–702.
- [16] C. Zhang, R.Z. Zuo, J. Zhang, Y. Wang, Structure-dependent microwave dielectric properties and middle temperature sintering of forsterite $(\text{Mg}_{1-x}\text{Ni}_x)_2\text{SiO}_4$ ceramics, *J. Am. Ceram. Soc.* 98 (3) (2015) 702–710.
- [17] R.Y. Yang, M.H. Weng, H. Kuan, TEM observation of liquid phase sintering in V_2O_5 modified $\text{Zr}_{0.8}\text{Sn}_{0.2}\text{TiO}_4$ microwave ceramics, *Ceram. Int.* 35 (1) (2009) 39–43.
- [18] X.S. Lyu, L.X. Li, H. Sun, S. Zhang, S. Li, High-Q microwave dielectrics in wolframite magnesium zirconium tantalate ceramics, *Ceram. Int.* 42 (1) (2016) 2036–2040.
- [19] R.D. Shannon, Dielectric polarizabilities of ions in oxides and fluorides, *J. Appl. Phys.* 73 (1) (1993) 348–366.
- [20] M.V. Jacob, D. Pamu, K.C.J. Raju, Cryogenic microwave dielectric properties of sintered $(\text{Zr}_{0.8}\text{Sn}_{0.2})\text{TiO}_4$ doped with CuO and ZnO, *J. Am. Ceram. Soc.* 90 (5) (2007) 1511–1514.
- [21] C.L. Huang, M.H. Weng, H.L. Chen, Effects of additives on microstructures and microwave dielectric properties of $(\text{Zr}, \text{Sn})\text{TiO}_4$ ceramics, *Mater. Chem. Phys.* 71 (1) (2001) 17–22.
- [22] R. Christoffersen, P.K. Davis, X. Wei, T. Negas, Effect of Sn substitution on cation ordering in $(\text{Zr}_{1-x}\text{Sn}_x)\text{TiO}_4$ microwave dielectric ceramics, *J. Am. Ceram. Soc.* 77 (6) (1994) 1441–1450.
- [23] A.E. McHale, R.S. Roth, Low-temperature phase-relationships in the system $\text{ZrO}_2-\text{TiO}_2$, *J. Am. Ceram. Soc.* 69 (11) (1986) 827–832.
- [24] S. Vahabzadeh, M.A. Golozar, F. Ashrafizadeh, Effect of annealing on microstructure of CuO-doped $(\text{Zr}_{0.8}\text{Sn}_{0.2})\text{TiO}_4$, *J. Alloy. Compd.* 509 (4) (2011) 1129–1132.
- [25] G.A. Ravi, F. Azough, R. Freer, Effect of Al_2O_3 on the structure and microwave dielectric properties of $\text{Ca}_{0.7}\text{Ti}_{0.7}\text{La}_{0.3}\text{Al}_{0.3}\text{O}_3$, *J. Eur. Ceram. Soc.* 27 (8–9) (2007) 2855–2859.
- [26] S.X. Zhang, J.B. Li, H.Z. Zhai, J.H. Dai, Low temperature sintering and dielectric properties of $(\text{Zr}_{0.8}\text{Sn}_{0.2})\text{TiO}_4$ microwave ceramics using $\text{La}_2\text{O}_3/\text{BaO}$ additives, *Mater. Chem. Phys.* 77 (2) (2002) 470–475.
- [27] A. Ioachim, M.G. Banciu, M.I. Toacsen, L. Nedelcu, D. Ghetu, H.V. Alexandru, C. Berbecaru, A. Dutu, G. Stoica, High-k Mg-doped ZST for microwave applications, *Appl. Surf. Sci.* 253 (1) (2006) 335–338.
- [28] W.T. Xie, H.Q. Zhou, H.K. Zhu, J.X. Zhao, G.W. Tang, X. Yu, Effect of $\text{ZnO}-\text{WO}_3$ additives on sintering behavior and microwave dielectric properties of $0.95\text{MgTiO}_3-0.05\text{CaTiO}_3$ ceramics, *Ceram. Int.* 40 (5) (2014) 6899–6902.